Hindawi
Adsorption Science & Technology
Volume 2022, Article ID 1384738, 16 pages
https://doi.org/10.1155/2022/1384738

Research Article

Multiresponse Optimization of Mechanical and Physical Adsorption Properties of Activated Natural Fibers Hybrid Composites

G. Velmurugan,[1] **V. Siva Shankar**,[1] **L. Natrayan**,[2] **S. Sekar**,[3] **Pravin P. Patil**,[4] **M. Senthil Kumar**,[5] **and Subash Thanappan**[6]

[1]*Institute of Agricultural Engineering, Saveetha School of Engineering, SIMATS, Chennai, Tamil Nadu 602 105, India*
[2]*Department of Mechanical Engineering, Saveetha School of Engineering, SIMATS, Chennai, 602105 Tamil Nadu, India*
[3]*Department of Mechanical Engineering, Rajalakshmi Engineering College, Rajalakshmi Nagar, Thandalam, Chennai, 602 105 Tamil Nadu, India*
[4]*Department of Mechanical Engineering, Graphic Era Deemed to be University, Bell Road, Clement Town, 248002 Dehradun, Uttarakhand, India*
[5]*School of Mechanical Engineering, Vellore Institute of Technology, Chennai, India*
[6]*Department of Civil Engineering, Ambo University, Ambo, Ethiopia*

Correspondence should be addressed to G. Velmurugan; velresearch032@gmail.com, L. Natrayan; natrayanmech007@gmail.com, M. Senthil Kumar; msv305@yahoo.co.in, and Subash Thanappan; thanappan.subash@ambou.edu.et

Received 29 April 2022; Revised 11 June 2022; Accepted 27 June 2022; Published 7 July 2022

Academic Editor: Jeevan Kumar Reddy Modigunta

In the current scenario, natural fiber-based biodegradable composites have increased because natural composite fibers are very cheap, biodegradable, lightweight, fireproof, and nontoxic. The present research work was carried out to optimize the mechanical properties of hybrid composites reinforced by Calotropis gigantea and hemp. To achieve these objectives, the following process parameters were determined, and RSM carried out optimization with the Box-Behnken experimental setup at three different levels: compression molding temperature (°C), pressure (bar), and time (min). The fibers were pretreated for 4 hours with a 5% NaOH solution to prevent moisture absorption. Regression equations were constructed to evaluate the mechanical properties, and the best process parameters were established. The results reveal that a pressure of 35 bar, a time duration of 7 minutes, and a temperature of 176°C are the best conditions for compression molding. The second aim was to compare CGF and hemp fiber-derived activated carbon adsorbents by determining physical adsorption properties, chemical compositions, and scanning electron microscope. Natural fibers were shown to be ideal candidates for manufacturing mesoporous activated carbon adsorbents with high surface area (1389–1433 m^2/g), high mesopore percentage (63–68%), and high carbon content (80–87%). Even though hemp activated carbon had a greater mesoporous structure (69%) than CGF-derived activated carbons, the CGF-derived activated carbons had larger surface areas and higher C content.

1. Introduction

The majority of engineering materials should be strong, rigid, and robust. Artificial composites are widely utilized to meet this need, owing to their ability to resist fracture, making them ideal for structural and semistructural applications. Natural fibers have gained popularity as an alternative to glass fibers in recent years, resulting in low specific gravity, low cost, and the ability to degrade completely. Natural fibers like wood, jute, flax, hemp, and kenaf are commonly used in the fabrication of automotive parts due to their low weight, low cost, reduced CO_2 emissions, and better recyclability [1–3]. Scientists, engineers, the general public, and governments worldwide are interested in developing

renewable and sustainable green composite materials from natural sources [4, 5]. Due to their immense potential as substitutes for fossil fuel plastic products, there has been a continual and ongoing investigation into the synthesis of innovative polymer materials from natural sources of crops and their compounds in recent decades. Scientists, engineers, the general public, and governments worldwide are interested in developing renewable and sustainable green composite materials from natural sources [6, 7]. Hemp (Cannabis sativa L.) is an ancient plant currently regarded as one of the most environmentally friendly commercial fibers. They can sometimes be misunderstood because they resemble the marijuana plant. However, unlike marijuana, hemp contains very little -9-tetrahydrocannabinol [8]. Hemp can be grown in temperate climates on a variety of well-drained, nonacidic soils with a high yield and no fertilizers or pesticides, reaching a height of 2-4 meters and a diameter of 5-16 millimeters. The hemp kernel is considered a low-value agricultural metabolic end due to its large hygroscopicity and lignin concentration.

High-quality hemp fibers with a cellulose-rich interface and increased personalization can be produced by further handling [9, 10]. Hemp fibers are contained in a matrix of hemicelluloses and lignin and structured into diverse architectural morphologies. Hemp fiber architecture has been thoroughly examined, resulting in useful, in-depth information available in contemporary literature. Single matrix composites with more than two fibers are known as hybrid composites. By addressing the drawbacks of individual composites, hybridization can help natural fiber-reinforced polymer composites have better mechanical characteristics [11]. Compared to other bast fibers, the Calotropis gigantea fibers (CGF) had a lesser elongation and better tensile characteristics and stiffness, allowing them to be used in polymeric composites as a substitute for manufactured fibers like glass and carbon. CGF has a greater lignin content than prior bast fibers, which gives more stiffness, and such fibers can be employed in lighter goods like clothing and automobiles due to their decreased density [12, 13].

Organic resources are not without flaws in quality, so they are not a problem-free alternative. Moisture can infiltrate through their structural arrangements (lignin, cellulose, gelatin, hemicelluloses, and waxy substances), resulting in poor coupling with matrix components. The surface of the fibers was modified using a variety of chemical treatments. NaOH is commonly used to change the interaction between different components, such as thermosetting polymers, raw fibers, and thermoplastic polymers. NaOH stimulates the hydroxyl groups, removing the wax and causing the outer cellulose fiber to shine [14, 15].

1.1. Physical Adsorption. Modern global warming indices have heightened public interest and participation in limiting the discharge of carbon dioxide. The rise in global temperatures, which began in the late 1800s, is anticipated to remain for an indefinite amount of time. Since the twentieth century, the average global temperature has risen by about 0.8 degrees Celsius. Numerous research has found that growing quantities of anthropogenic emissions and polycyclic aromatic hydrocarbons created by actions like burning fossil fuels contribute to "climate change." Since these gases can absorb, emit, and reabsorb sunrays, they are anticipated to contribute significantly to global warming via the greenhouse effect. Carbon dioxide is responsible for 80% of greenhouse gas emissions, contributing to global warming. As a result, limiting CO_2 emissions is crucial for reducing the greenhouse effect [16, 17]. Physical and chemical stimulation could be used to create activated carbon. Physical activation is done in 2 stages: (1) carbonization of the precursor material and (2) gasification of the char in a steam or carbon dioxide atmosphere. Biochemical initiation is accomplished in a solitary phase that integrates the carbonization processes, resulting in improved porosity structures. It is also carried out at a reduced heat transformation compared to physical stimulation.

On the other hand, the chemical activation procedure has the drawbacks of being caustic and requiring a cleaning stage [18, 19]. Chemical activation was chosen for this project due to its numerous energy-saving advantages. The percentage of the active catalyst, which has been investigated in the literature at roughly 35–80%, is one of the most critical criteria for the chemical method. One of the goals of this research was to minimize the activation chemical and hence lower the cost of activated carbon production. Because pore size contributes significantly to adsorption, selecting the optimum activated charcoal pore size is particularly critical [20, 21]. Adsorbate gas molecules with diameters of more than two nanometers, for example, were readily adsorbed in mesopores (2–50 nm) but not in micropores. Even though highly mesoporous activated carbons are desirable for specific applications like the transformation of energy, wastewater handling plants, stowage resources, and bioengineering substantial claims, mesoporous triggered carbons have received less attention in the literature due to their expensive and complicated fabrication method [22, 23].

RSM stands for response surface methodology, a set of mathematical and statistical approaches for creating, enhancing, and optimizing the process parameters. It is a two- or three-dimensional hypersurface approach for determining and displaying the cause-and-effect connection between responses and input control factors influencing outputs. For RSM, the Box-Behnken design (BBD) is considered an experimental design. BBD has a significant advantage in avoiding tests conducted in extreme environments. It does not include combinations in which all elements are at their greatest or lowest values simultaneously. Furthermore, the BBD is often used in industrial research since it is a cost-effective design requiring only three levels for each component. Thermoplastic composites are commonly produced through compression molding. Massive, compact, robust, durable, and low-weight composites may be made using this approach. The major benefit of compression molding would be that the natural fibers would not be sheared, making it easier to minimize fiber damage [24]. The compression molding processing parameters significantly impact the composites' properties and interfacial features, and they largely determine the final product's quality. Temperature, pressure, and heating time are the most significant

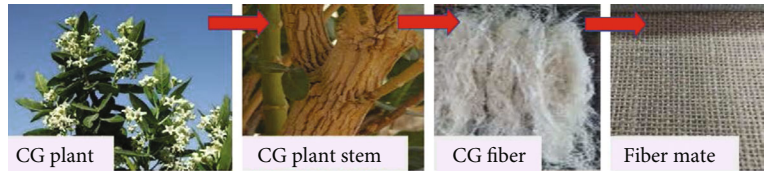

Figure 1: Extraction of Calotropis gigantea fiber (CGF) from Calotropis gigantea plant.

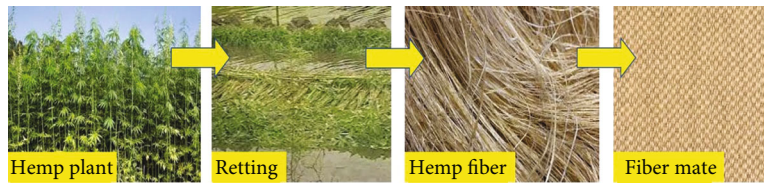

Figure 2: Extraction of hemp fiber from hemp plant.

compression molding process factors that impact mechanical characteristics. As a result, to produce the best composite goods, the right processing parameters must be carefully chosen.

No reports highlight the use of RSM with desirability functions to fabricate composites from CGF and hemp fiber. The primary focus of this investigation is to improve the compression molding process for CGF and hemp-based polypropylene composites in terms of mechanical characteristics. The secondary goals of the study are to develop cost-effective methods of producing and characterizing mesoporous activated carbons from natural fibers such as CGF and hemp. One way of lowering the cost was to impregnate natural fibers with a small concentration of an activating agent. The Box-Behnken design setup with the RSM approach was used to attain the above-mentioned objective.

2. Materials and Method

2.1. Materials. Calotropis gigantea (CGF) and hemp are two South Asian shrubs that may be found in abundance in India, Thailand, and Malaysia. A retting technique removes fibers from the plant's stem bark. It is first separated into small strands of up to one meter, which are then converted into a woven mat. The reinforcements like CGF and hemp were gathered in the Jute service center in Madurai, Tamil Nadu, India. Photographic images of CG fiber and hemp fiber are shown in Figures 1 and 2. Table 1 lists the mechanical properties of CGF and hemp fibers.

2.2. Alkaline Treatment. To eliminate any unwanted contamination of the raw hemp and CG fibers will be cleaned separately at 60 to 75°C for 1 hour with 1 to 2% detergent solutions, then rinsed with refined (distilled) water, and cured in a vacuum oven at 70°C for 1 hour 30 minutes, as per the elaborated technique [25]. The cleaned fibers were then submerged in 5% solutions of NaOH for 4 hours at 30°C. To obtain the alkali-treated fibers, they were completely cleaned with distilled water and dried by ambient air.

Table 1: Mechanical properties of reinforcements used in the current research.

Sl. no	Properties	Calotropis gigantea fiber	Hemp fiber
1	Density (g/cm^3)	0.56	1.5
2	Tensile strength (MPa)	381	690
3	Young's modulus (GPa)	9.7	70
4	Elongation (%)	2.1	1.6

2.3. Adsorption Methods. For many decades, granulated activated carbons (GAC) were the industry's norm as adsorbents in air circulation systems and air-purifying respirators to remove gas-phase pollutants. GAC provides an expensive, elevated solution for recovering pure products for recycling. Granulated activated carbon may be made into a module which can be extracted, regenerated, and reused after exhaustion. In this study, natural fiber adsorbents were made by carbonizing and physically activating the carbonized fibers. In the adsorption system, the surface area of an adsorbent is critical. The larger the surface area, the greater the adsorption capacity. The surface area was calculated using a Micromeritics ASAP 2020 automated physical adsorption analyzer using isotherm plots of nitrogen adsorption by the samples at 77 K in the relative pressure range (P/P0) from 0.02 to 1. In the apparatus, all of the samples were degassed and analyzed. The dewatering procedure, carried out at 300°C for 1 hour of analysis, pretreats the adsorbent specimen by using a combination of heating, pressure, and/or flowing gas to eliminate adsorption pollutants from atmospheric exposure. The adsorbent specimens are incrementally dosed with nitrogen during the analytical procedure.

The amount of nitrogen necessary to create a monolayer across the adsorbent's exterior surface and pores was calculated at various pressures. The surface area was determined using the area surrounded by each adsorbed nitrogen gas molecule. It is crucial to examine the complete pore structure of an adsorbent since hole dimensions impact the adsorption behavior of molecules of diverse forms and

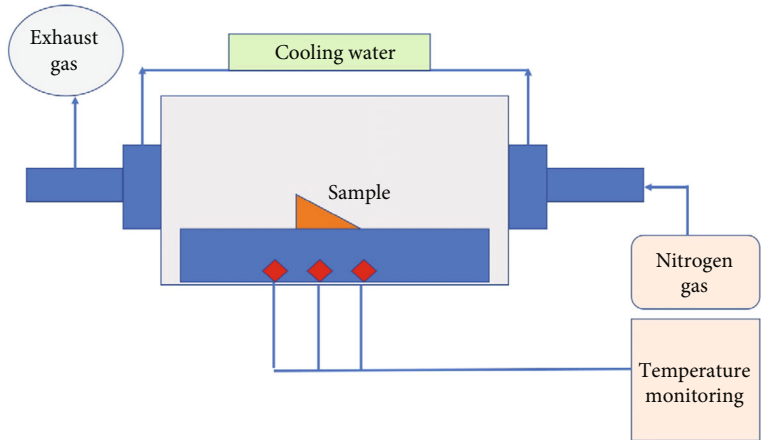

Figure 3: Horizontal furnace setup of natural fiber activated carbon process.

dimensions. Hole proportions have been one of the factors used to choose carbon adsorbent materials for a certain purpose [26]. Figure 3 shows the schematic arrangement of the horizontal furnace.

2.4. Ultimate and Proximate Examination. The strength of the biobased composites mainly depends on the various chemical ingredients or elements like hydrogen, carbon, and nitrogen. These can be measured by using the ultimate examination method. It can be performed using a Perkin Elmer CHN analyzer. At the same time, the concentrations of moisture content, volatile matter, ash content, and fixed carbon were restrained by using close examination. The percentage of static content in the carbon is indicated by the amount of ash present in the fibers. Typically, natural-based composite specimens have a 2% ash content. Because the adsorption rate of the activated carbon specimen is poor, a high ash concentration is undesirable. Adsorbent will be minimal if the humidity level is high, which will raise shipping and storage expenses. The commercially available activated specimens have a 5–8% water content. Activated carbon is a good choice for adsorption research since it has a low ash level and a low moisture content. The existence of biological components in the sample is indicated by volatile matter [27, 28].

3. Experimental Works

3.1. Fabrication and Testing of Hybrid Materials. A laboratory-scale blending machine mixed the scouring CGF, hemp, and polypropylene fibers at 15, 30, and 50 weight ratios. The natural fiber hybrid composites were produced in a compression molding machine using the BBD design of the experiment, with temperatures of 164, 174, and 184°C; pressures of 34, 40, and 45 bar; and heating times of 6, 11, and 15 minutes. Seventeen plates are manufactured according to the BBD design. Mechanical specimens are made utilizing the fabricated composite as per ASTM specifications. Tensile tests on the composite specimens were done using a UTM machine at 2 mm/min cross-head speed under ASTM D3039 (25 × 250 mm). At the same cross-head speed, flexural testing was carried out on the same machine by ASTM D790-10 (12.7 × 125 mm). The composite samples were also submitted for impact testing under ASTM D256-10 utilizing an impact tester (64 × 12.7 mm). Figure 4 shows the specimen size of mechanical characterization.

3.2. Design of Experiment. RSM is a tool for evaluating the relationships between a set of controlled circumstances and observable outcomes. To create a statistical model, you must first understand the process. This method has been described in great depth [29, 30]. The three key phases in this optimization process are conducting scientifically planned trials, predicting the constants in a scientific method, forecasting the responses, and verifying the model's appropriateness. Significant factors such as pressure, time, and temperature were chosen as crucial factors and correspondingly given the numbers Y1, Y2, and Y3. Multiregression analysis with the least-squares approach was used for

$$i = \frac{y_i - y_0}{\Delta y}, \text{ where } i = 1, 2, 3 \tag{1}$$

In the above equations, Yi is the coded value of self-determining factors, y_i is the real value of a self-determining factor, y_0 is the genuine value of a self-determining factor based on the midpoint, and y is the self-determining factors modification standards. A collection of spots lies only at the midway point between every edge and the duplicated midpoint of the dimensional block in the Box-Behnken design. All tests were repeated three times, with the mean of the processing conditions yields used as the outcome. The mathematical relationship of the response to such parameters in an arrangement with 3 major self-determining factors (Y1, Y2, and Y3) may be represented by the quadratic equation:

$$X = \partial_0 + \partial_1 Z_1 + \partial_2 Z_2 + \partial_3 Z_3 + \partial_{11} {Z_1}^2 + \partial_{22} {Z_2}^2 + \partial_{33} {Z_3}^2 + \partial_{12} Z_1 Z_2 + \partial_{13} Z_1 Z_3 + \partial_{23} Z_2 Z_3 + \in . \tag{2}$$

X is the anticipated reaction; $\alpha 0$ is the model constants; Z_1, Z_2, and Z_3 are significant factors; 1, 2, and 3 are linear

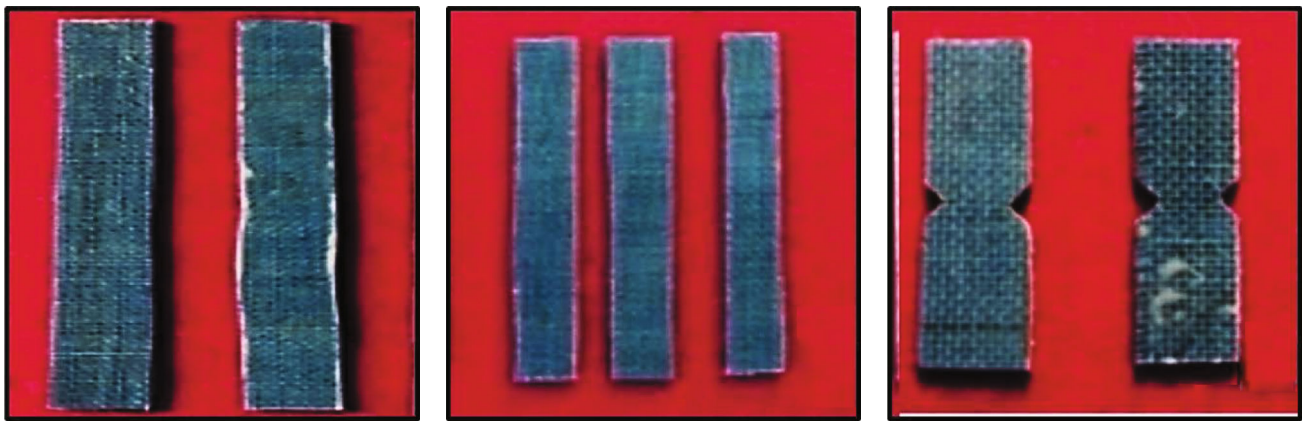

(a) (b) (c)

Figure 4: Specimen size of (a) tensile, (b) flexural, and (c) impact strength.

constants; 12, 13, and 23 are product cross order constants; 11, 22, and 33 are quadratic constants; and 1, 2, and 3 are linear constants. The factor of fortitude, R^2, was utilized to describe the degree of fit of the polynomial model calculation. The melting point of the phenol-formaldehyde applied in this research was used to control the amounts of factors such as pressure, time, and temperature. The coefficients are obtained by multiple regression analysis, and the calculation may be utilized to find the outcomes. Box-Behnken, a fractional factorial setup with three factors, was selected as the degree of experimentation for this investigation [31].

3.3. Preparation of Activated Carbons. CGF and hemp natural fibers were used as carbon precursors. This study used a 20-weight-percent activating agent to save money and energy. The chemical activation agent was phosphoric acid (H3PO4). Because of its ease of retrieval through water cleaning, H3PO4 is frequently employed in literature. This also works as a dehydrator and prevents the production of asphalt. For 1 hour, H3PO4 was injected into natural fiber precursors. A flat heater was employed for carbon production throughout the carbonization procedure, as designated in Figure 3. The furnace had a 6 cm inner diameter, a length of 110 cm, and a three-zone temperature control mechanism to manage its temperature. The model substantial was kept in the center of the heater, and the arrangement was then erased with nitrogen gas at a flow rate of 93.3 ml/min for 1 hour of the lodge period, with a heating rate of 10°C/min. The cleaning solutions, like hydrochloric acid, purified water, and warm water, were all used to wash the final product. The cleaned specimen was then dried for 2 hours at 100 degrees Celsius [28].

4. Outcomes of Hybrid Composites

4.1. Tensile Properties. The tensile behaviors of CGF- and hemp-based natural composites are depicted in Figures 5(a)–5(c) depending on various factors. It has been shown that whenever the temperatures of compression molding climb to 173°C to 175°C, the tensile behaviors rise as well, before progressively declining. This might be related to the CGF fibers' heat deterioration. Thermal decomposition of hybrid composites results in a nonreversible loss of fiber goodness, which invariably affects the tensile characteristics. At approximately 54°C, moisture desertion by warmth causes significant loss in CGF- and hemp-based hybrid composites, and thermal breakdown of fibers occurs at approximately 231°C [32].

The material's tensile strength decreases initially as the molding time rises but then progressively increases. This might be due to the material's partial stress relief. It is also evident that as the molding pressure rises, hybrid composites' tension behaviors fall at first and then rise.

4.2. Flexural Properties. The flexural behaviors of CGF- and hemp-based hybrid composites are depicted in Figures 6(a)–6(c) dependent on various variables. When the temperature rises, the flexural behaviors of hybrid composites improve; the flexural strength improves as well, reaching 174°C before gradually decreasing due to thermal deterioration of CGF fibers. The flexural strength initially drops and subsequently increases as the holding time in the mold increases. A significant trend of duration and pressure can be noticed in flexural behaviors.

4.3. Impact Strength. Figure 7(a) shows the impact strength with response surface plots for pressures of 33 to 44 bar and holding times in the molds of 6 to 13 min. Figure 7(b) shows outcome-based surface plots of the impact behaviors of CGF- and hemp-based hybrid composites for compression pressures ranging from 33 to 44 bar and temperatures ranging from 164 to 180°C. The response surface plots for impact strength of CGF- and hemp-reinforced hybrid composites molded at temperatures ranging from 164 to 180°C and times ranging from 6 to 15 minutes are shown in Figure 7(c). The impact strength of hybrid composites improves with the temperature and then progressively decreases due to thermal deterioration. It can be seen that when the holding time in mold increases, the impact properties decrease. This might be due to the material's partial

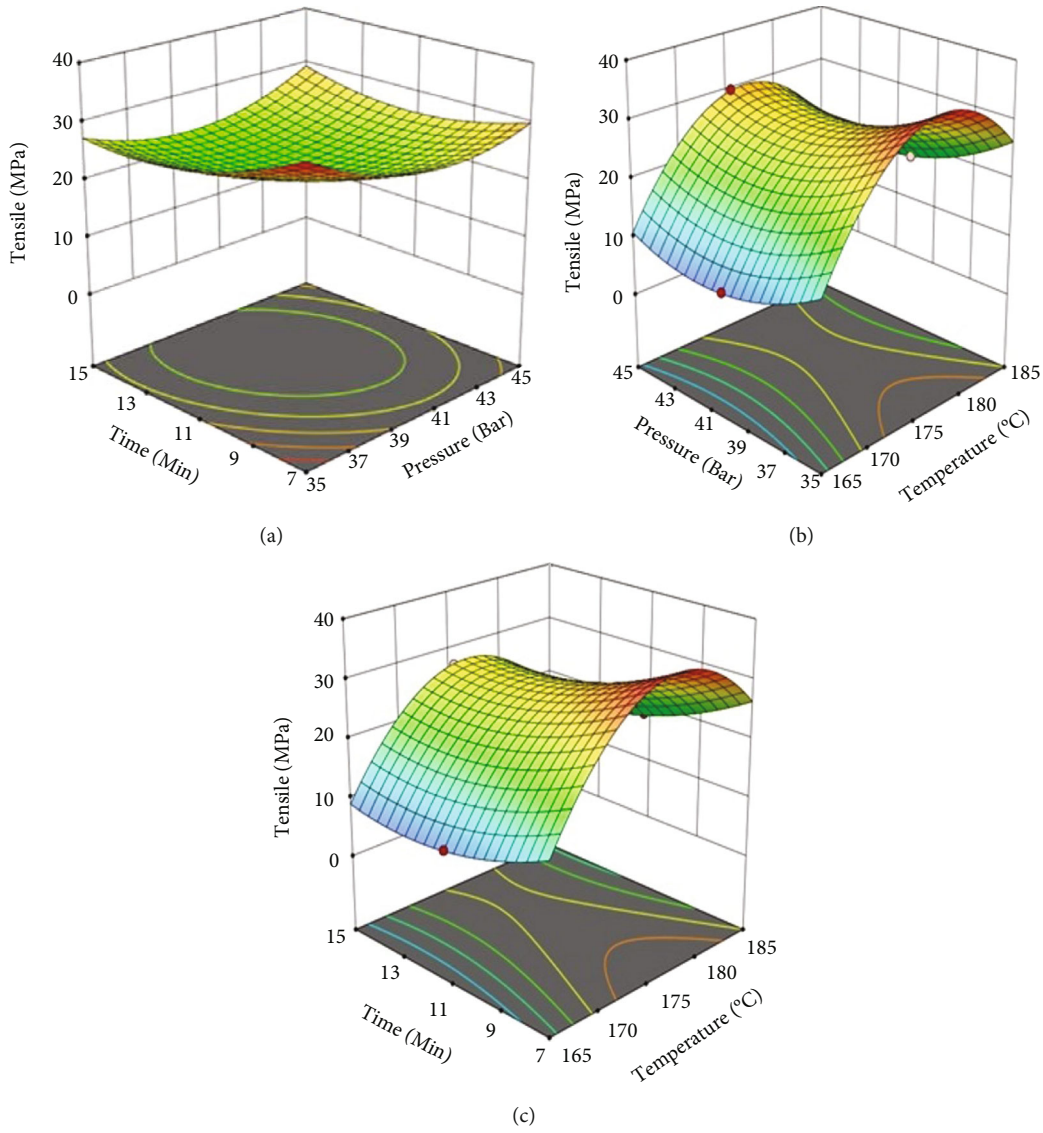

Figure 5: Tensile behavior of (a) pressure vs. time; (b) temperature vs. pressure; (c) temperature vs. time of CGF- and hemp-based hybrid composites.

stress relief. It is also worth noting that the impact strength decreases when the molding pressure rises. This is mostly because increased molding pressure causes the structure to become more compact, creating a larger crystalline area, which contributes to the composite's reduced impact strength [33]. The CGF and woven hemp fibers were chemically pretreated with a 5% sodium hydroxide (NaOH) formulation for 4 hours to extract hydrophilic hydroxyl groups and contaminants from wood and jute cellulose fibers. This will improve fiber adhesion and durability even with the polyester matrix. This increases the levels of the polymerization reaction and the fibers' crystalline structure, which substantially improves the mechanical and morphological characterization.

4.4. Response Surface Models. The below session explains the RSM model for mechanical properties of hemp- and CGF-based hybrid composites as a purpose of the compression molding process parameter. It demonstrates the models' appropriateness and the accuracy of the derived factor. Tensile, flexural, and impact strength correlation coefficient values (R^2) are correspondingly 0.96, 0.97, and 0.96. The correlations between tensile behavior and their factors account for data erraticism.

$$\begin{aligned} \textit{Tensile Strength} = {} & 21.96 + 4.01Y_1 - 0.7938Y_2 - 2.03Y_3 \\ & - 0.7425Y_1Y_2 - 1.06Y_1Y_3 + 1.95Y_2Y_3 \\ & - 14.49{Y_1}^2 + 5.01{Y_2}^2 + 3.39{Y_3}^2, \end{aligned}$$

$$\begin{aligned} \textit{Flexural Strength} = {} & 24.68 + 4.79Y_1 - 1.75Y_2 - 2.62Y_3 \\ & - 1.53Y_1Y_2 - 1.94Y_1Y_3 + 1.16Y_2Y_3 \\ & - 15.82{Y_1}^2 + 4.90{Y_2}^2 + 3.18{Y_3}^2, \end{aligned}$$

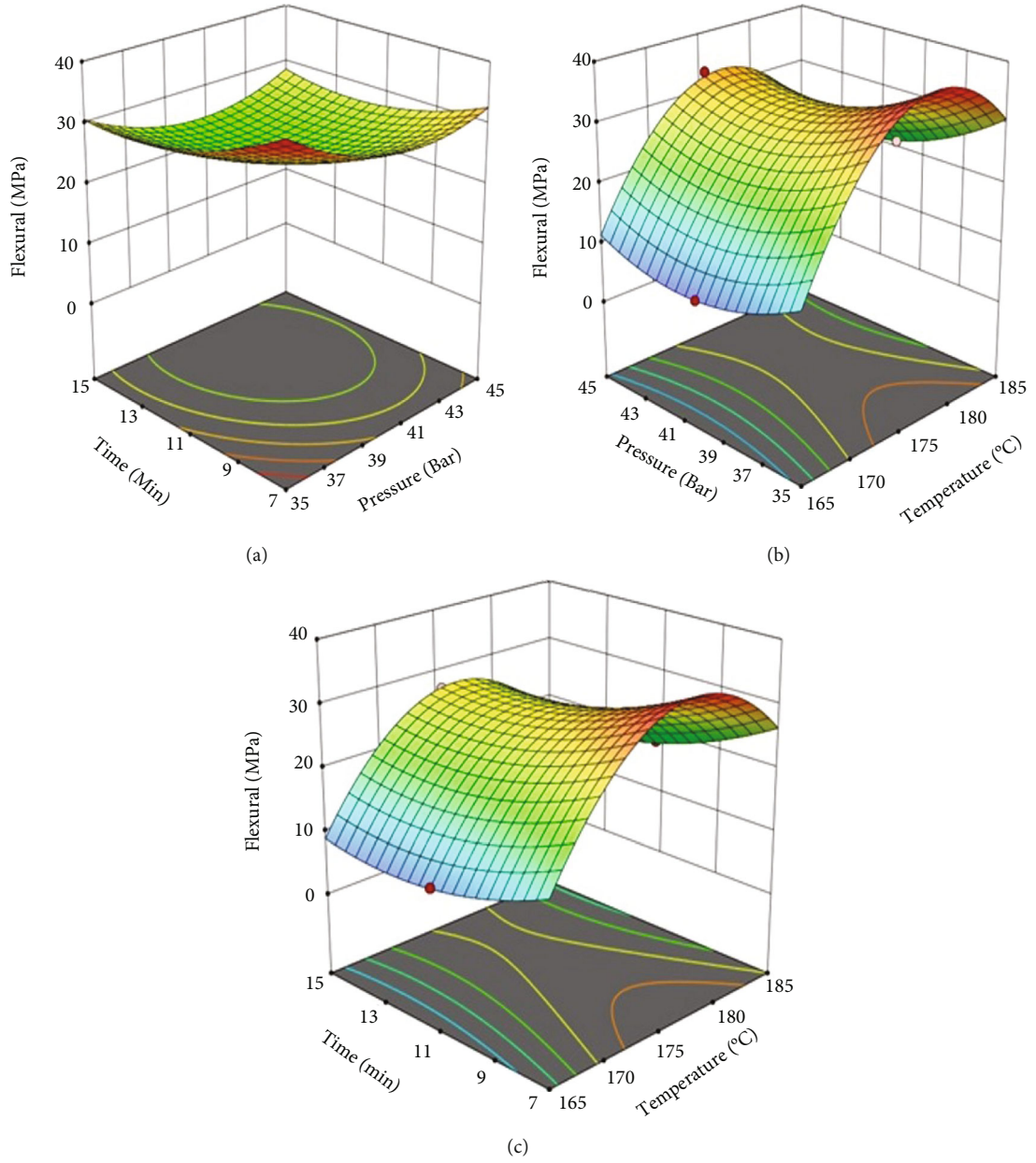

Figure 6: Flexural behavior of (a) pressure vs. time; (b) temperature vs. pressure; (c) temperature vs. time of CGF- and hemp-based hybrid composites.

$$\begin{aligned} \textit{Impact Strength} = {} & 2.08 + 0.0685Y_1 - 0.1575Y_2 + 0.0590Y_3 \\ & + 0.0380Y_1Y_2 - 0.1765Y_1Y_3 - 0.1565Y_2Y_3 \\ & - 0.90{Y_1}^2 - 0.060{Y_2}^2 - 0.046{Y_3}^2. \end{aligned} \tag{3}$$

4.5. Analysis of Developed Mathematical Models. Tables 1–3 show the results of an analysis of variance (ANOVA) for the mechanical properties of the hybrid composites. The ANOVA technique normally helps to regulate the sufficiency and relevance of the RSM model and its factors. The model's appropriateness is assessed using the F value. Table 2 shows that the quadratic model is appropriate for predicting tensile strength, with a model F value of 1093.24. According to this table, the quadratic model's "Prob > F" value is less than 0.0001, indicating that the model is substantial. Furthermore, the major impacts of temperature (A), time (c), pressure and time interaction (BC), and the product of temperature (A^2), pressure (B^2), and time (C^2) are all significant models variables.

Table 3 shows that the quadratic model is appropriate for predicting flexural strength, with a model F value of 46.90. According to this table, the quadratic model's "Prob > F" value is less than 0.0001, indicating that the model is substantial. Furthermore, the temperature (A^2) model's product is significant. Table 4 shows that the quadratic model is appropriate for predicting impact strength, with a model F value of 38.12. According to this table, the

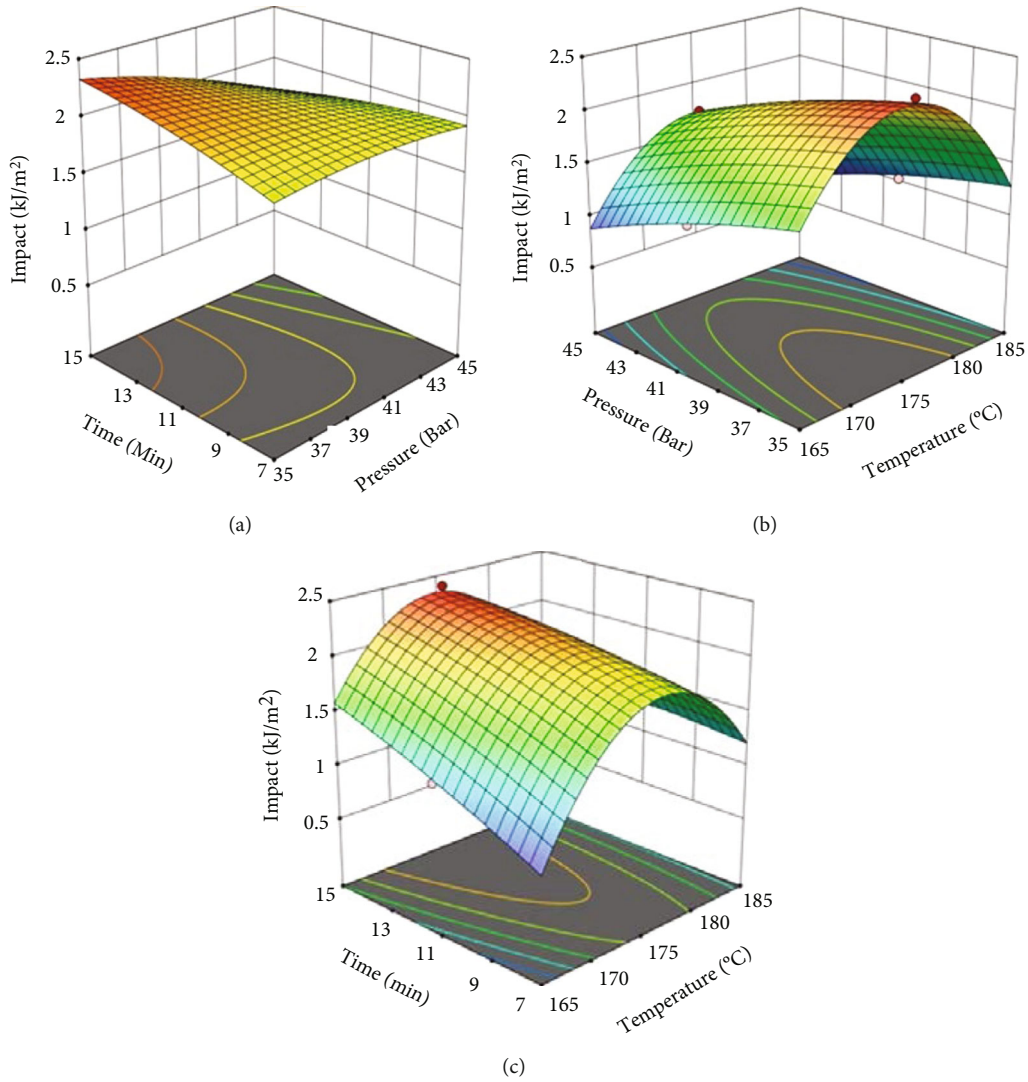

Figure 7: Impact behavior of (a) pressure vs. time; (b) temperature vs. pressure; (c) temperature vs. time of CGF- and hemp-based hybrid composites.

Table 2: ANOVA for tensile strength.

Source	Sum of square	df	Mean square	*F* value	*p* value
Model	1183.86	9	131.54	1093.24	<0.0001
A-temperature	128.72	1	128.72	1069.82	<0.0001
B-pressure	5.04	1	5.04	41.89	0.0003
C-time	32.97	1	32.97	273.99	<0.0001
AB	2.21	1	2.21	18.33	0.0037
AC	4.45	1	4.45	37.00	0.0005
BC	15.29	1	15.29	127.06	<0.0001
A^2	884.44	1	884.44	7350.68	<0.0001
B^2	105.55	1	105.55	877.22	<0.0001
C^2	48.37	1	48.37	401.98	<0.0001
Residual	0.8422	7	0.1203		
Cor total	1184.70	16			

Table 3: ANOVA for flexural strength.

Source	Sum of squares	df	Mean square	F value	p value
Model	1445.14	9	160.57	46.90	<0.0001
A-temperature	183.74	1	183.74	53.67	0.0002
B-pressure	24.51	1	24.51	7.16	0.0317
C-time	54.87	1	54.87	16.03	0.0052
AB	9.31	1	9.31	2.72	0.1430
AC	15.08	1	15.08	4.40	0.0740
BC	5.41	1	5.41	1.58	0.2492
A^2	1054.40	1	1054.40	307.99	<0.0001
B^2	101.11	1	101.11	29.53	0.0010
C^2	42.47	1	42.47	12.40	0.0097
Residual	23.96	7	3.42		
Cor total	1469.10	16			

Table 4: ANOVA for impact strength.

Source	Sum of squares	df	Mean square	F value	p value
Model	4.05	9	0.4504	38.12	<0.0001
A-temperature	0.0375	1	0.0375	3.18	0.1179
B-pressure	0.1984	1	0.1984	16.80	0.0046
C-time	0.0278	1	0.0278	2.36	0.1686
AB	0.0058	1	0.0058	0.4888	0.5070
AC	0.1246	1	0.1246	10.55	0.0141
BC	0.0980	1	0.0980	8.29	0.0237
A^2	3.47	1	3.47	293.61	<0.0001
B^2	0.0155	1	0.0155	1.31	0.2895
C^2	0.0090	1	0.0090	0.7606	0.4120
Residual	0.0827	7	0.0118		
Cor total	4.14	16			

quadratic model's "Prob > F" value is less than 0.0001, indicating that the model is substantial. Furthermore, the pressure (B^2) model's product is significant. Aside from the models mentioned above, a few more are not obvious.

The appropriateness of the model is assessed using a normal probability plot for residuals, which evaluates the data used in the model for composite properties. Figure 8 shows the normal predicted vs. actual graphs for residuals of composite properties. The random and normally distributed residuals show the absence of any predictive information in the mistake. The residual sin prediction response is small because they are so close to the diagonal line. As a result, the deterministic part of the model does a decent job of describing the elasticity modulus, leaving just the intrinsic randomness in the error part [24].

4.6. Adsorption Results. Table 5 lists the surface area measurements for native fibers, carbonized specimens, and activated specimens. All carbonized specimens had a burn-off proportion of 60-69%, whereas activated specimens had a burn-off proportion of 50–60%. The form of the isotherm models in Figure 9 is type I, exhibiting the Langmuir-type monolayer adsorption typical of microporous adsorbent materials, as per the nitrogen adsorption-desorption curve [16].

4.6.1. Surface Area and Pore Characteristics. For activated carbon fields such as industrial emissions purifying, water purifying, and storage tank purposes, large surface ranges (>1100 m^2/g) are essential to increase pollutant collection competence. The higher surface area usually equates to greater adsorption capability. However, the adsorption capacity of activated carbon is also influenced by pore size and volume [34]. The pore size properties determine the dimension of the contaminant elements that the carbon may absorb. The amount of adsorbate is determined by the volume of the pores. The shape of the adsorption isotherm offers qualitative data about the adsorption process and surface area. The existence of micropores and mesoporous in activated carbon, in particular, boosts their adsorption

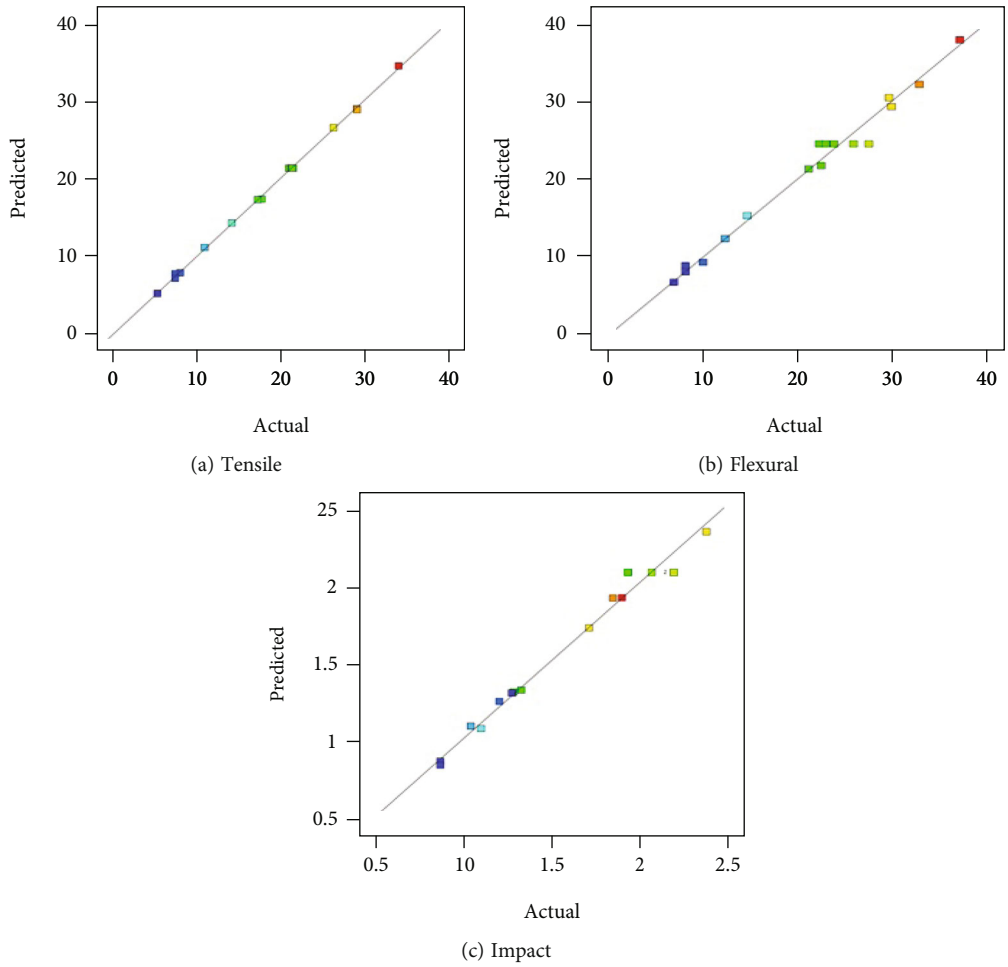

Figure 8: Predicted vs. actual value of (a) tensile, (b) flexural, and (c) impact strength of CGF- and hemp-based hybrid composites.

Table 5: CGF- and hemp-based activated carbon adsorbents characteristics ($n = 3$).

Sample	BET surface area (m^2/g)	Micropore surface (m^2/g)	Mesopore surface (m^2/g)	Percentage (%)
CGF	1433	469	987	68.87
Hemp	1389	412	966	69.54

capability for bigger adsorbed molecules [35]. The mesopore surface area, surface morphology, micropore surface area, mesopore volume, total pore volume, micropore volume, and pore size of activated carbon formed by H_3PO_4 chemical CGF- and hemp-derived specimens, sequentially, are summarized in Table 5. According to the data, the CGF- and hemp-derived activated carbons had the highest surface range (1200–1400 m^2/g) and the highest mesopore concentration (60–70%). Activated carbons obtained from natural fibers can therefore be used to create a mesoporous structure with a large surface area. With chemical activation, Dev et al. [36] reported mesoporous assembly. For each of these adsorbents, mesopore volume, the mesopore area ratio, total pore volume, and pore diameters micropore volume altered slightly. The maximum BET surface range (1433 m^2/g) was achieved from CGF-derived activated carbon, although hemp-derived activated carbon had the highest microporosity (60.27 percent). BET surface ranges and their total volume are directly related to each other, as shown in Table 5, with BET surface area rising as micropore range, mesopore range, and total volume of pore increase. On the other hand, BET surface ranges were contrariwise related to hole dimensions. The normal hole diameters of activated carbons made from CGF (1433 m^2/g) and hemp (1389 m^2/g) were 2.12 and 2.29 nanometers, respectively. It also demonstrates that the chemical activator generates porosity and expands pores, forming a mesoporous structure. Table 6 lists the above findings.

The micropore size distribution for organic fiber-derived activated carbons is shown in Figure 10. All varieties of activated carbon have a wide range of micropore sizes. The preponderance of micropores was between 0.5 and 0.6 nanometers, but the models also included a minor peak between 0.7 and 0.9 nanometers.

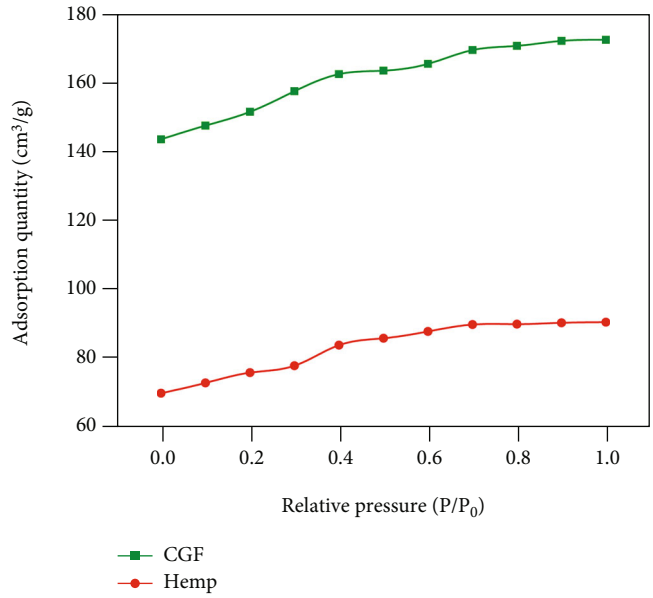

Figure 9: CGF and hemp-based bio composites under N_2 adsorption.

Table 6: Pore diameter measurement of natural fiber based on adsorbent characteristics.

Sample	Total volume (cm^3/g)	Micropore volume (cm^3/g)	Mesopore volume (cm^3/g)	Percentage (%)	Pore size (nm)
CGF	0.79	0.33	0.47	59.49	2.12
Hemp	0.73	0.29	0.44	60.27	2.29

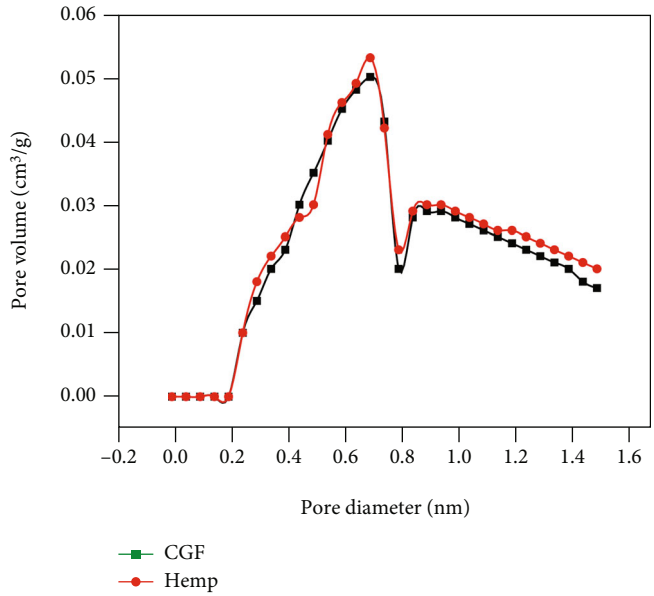

Figure 10: Micropore distribution of CGF and hemp activated carbon.

4.6.2. Proximate and Ultimate Investigation. In most cases, the final analysis identifies the element composition of the material, like the proportions of carbon, nitrogen, and hydrogen. However, because the apparatus employed in this study (Perkin-Elmer CHN 2400) could only measure hydrogen, carbon, and nitrogen, the alteration may also be S or O or a combined effect of S and O. The findings of the ultimate and proximate studies of activated carbons produced from CGF and hemp are summarized in Figure 11(a). It can be shown that the specimen is mostly composed of C greater

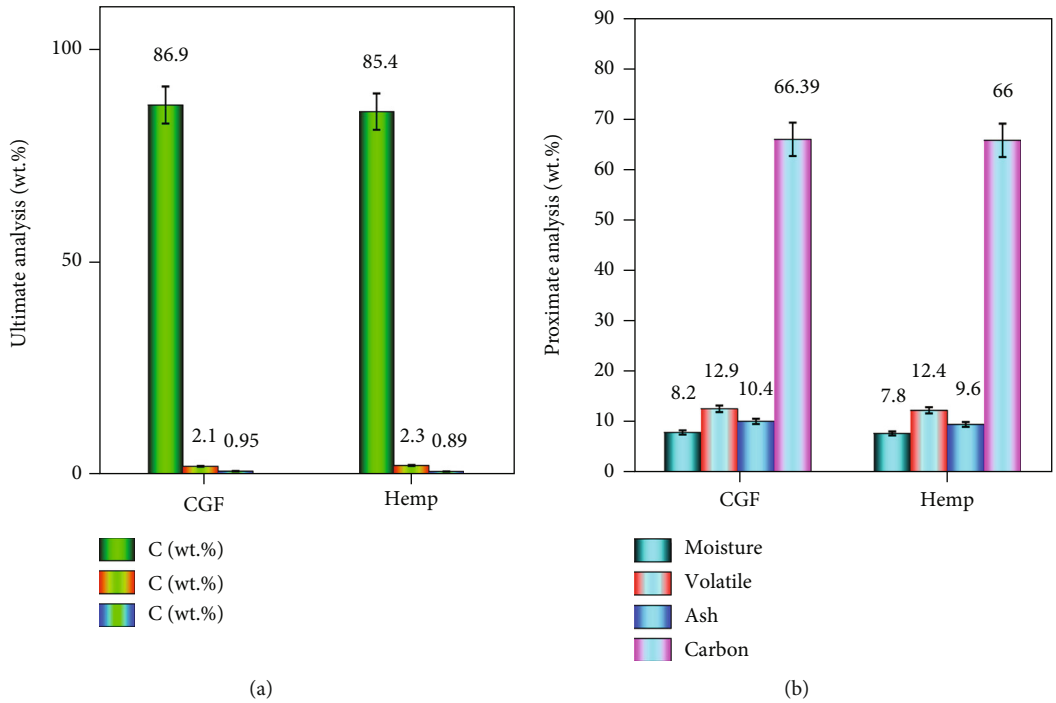

Figure 11: (a) Ultimate analysis; (b) proximate analysis of CGF and hemp-based natural fibers.

than 85%, with 2–2.5 percent H and 0.8 to 0.9 percent N. The quantity of fixed carbon was smaller than the amount of elemental carbon in each sample, and the fixed carbon value was comparable to the amount of rudimentary carbon. The proximate examination findings suggest that fixed carbon (80–87%) is the predominant component, with volatile matter, ash, and moisture content accounting for the rest (30–40%). CGF-derived AC has the highest C (68 wt%) and fixed carbon content (66.39 wt%). The final examination and fixed carbon proportion consequences for hemp-derived activated carbon were quite close to those for flax-derived activated carbon, indicating that the qualities of the raw material and natural fiber are identical (Figure 11(b)).

5. Fractographic Studies

5.1. Mechanical Testing. A scanning electron microscope was used to perform a morphological examination. After completing experiments, the surface properties of the CGF- and hemp-based hybrid composite materials were investigated using SEM. A Zeiss SUPRA 55-VP scanning electron microscope (SEM) was used to perform microscopic analyses of broken composite specimens at Sathyabama University, Chennai. To improve the composite's electrical conductivity, it has been washed, dried, and surface covered by 10 nm of gold past the SEM clarification. SEM images vividly show the interfacial bonding among the hybrid composites. The adherence of fiber and resin in a hybrid composite subjected to tensile testing is shown in Figure 12(a). The adhesion is generally good. However, there are some flaws, like air bubbles, and fiber pull-out.

The reason for this might be the inadequate matrix and fiber mixing, which causes poor wettability between fibers and the matrix, resulting in a matrix fracture [37]. Hybrid composites' thermal breakdown reduces the composite strength through fiber damage, which always impacts the composites' tensile properties [38]. The high-stress values observed in the test suggest good stress transmission in the tensile direction between reinforcement and resin [39]. An SEM image of a flexural cracked composite is shown in Figure 12(b). The cross-section of the applied force shows interphase debonding. Due to the consistent weight applied to the specimen, the existence of voids is negligible. The degree of breakage of CGF and hemp in the hybrid composite subjected to impact testing is shown in Figure 12(c). The fibers are shattered due to the abrupt impact, but there is no evidence of fatigue failure [40]. Furthermore, due to the woven structure of the fiber, it is evident that there is a homogeneous distribution throughout the matrix, as well as enough interfacial adhesion [41]. It will confirm the effectiveness of NaOH treatment (5% NaOH for 4 hrs). Matrix breakage reduces the mechanical characteristics of hybrid composites. It occurred as a result of thermal decomposition [42]. The SEM picture also shows the need to control compression molding factors like time, pressure, and temperature.

5.2. Microstructural Analysis of Activated Carbons. The porosity microstructure seen in organic fiber-derived activated carbons was investigated using SEM. Well-developed pores were visible on the exterior of all organic fiber-derived ACAs [43]. These findings show that the cross-sectional area of adsorbents remained inhomogeneous

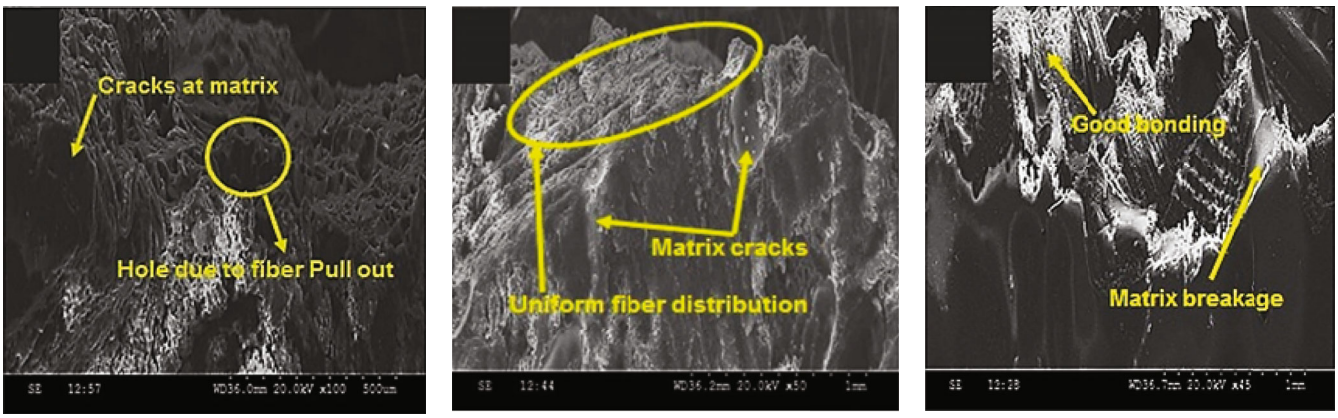

(a) (b) (c)

Figure 12: Microstructural image of fractured specimen after (a) tensile; (b) flexural; (c) impact testing.

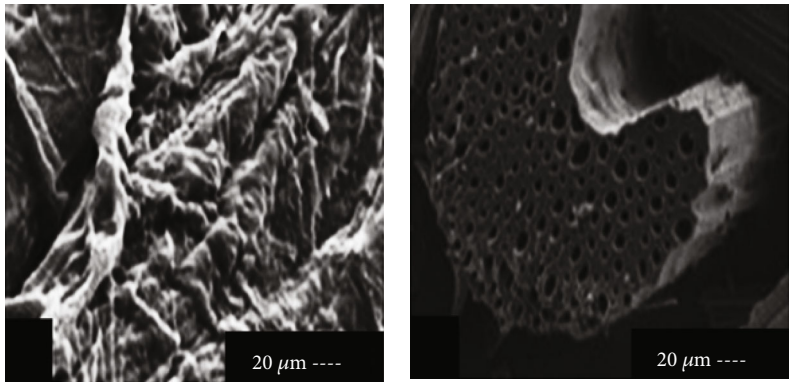

(a) (b)

Figure 13: CGF activated carbons (a) longitudinal surface; (b) cross section.

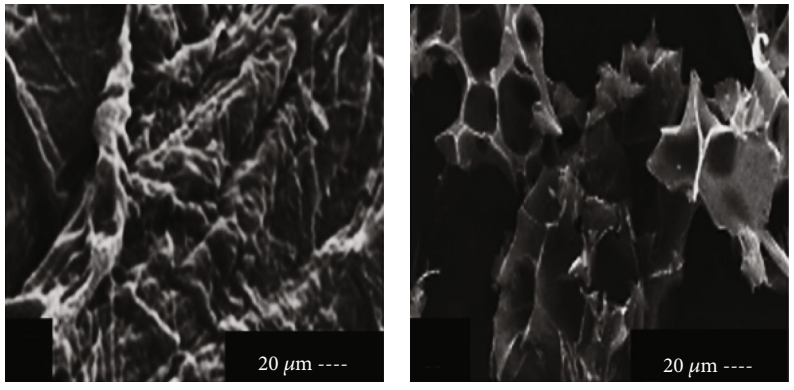

(a) (b)

Figure 14: Hemp activated carbons (a) longitudinal surface; (b) cross section.

during the carbonization and activation stages, with a broad diversity of egg-shaped holes [44]. Some particles were discovered on the specimen surface, which could be remnants left over from the carbonization or activating stages [45]. The number of holes and pore size distribution of activated carbon vary greatly depending on the kind of natural fiber [46]. Furthermore, SEM reveals diverse and uneven pore diameters [47, 48]. Figures 13 and 14(a) and 14(b) depict the longitudinal and cross sections of activated carbons from a CGF and hemp fiber, respectively.

6. Conclusion

The optimization of hemp- and Calotropis gigantea (CGF)-reinforced polypropylene composites concerning mechanical properties was done using the design setup of Box-Behnken and RSM.

(i) The findings of this investigation show that mold temperature has the greatest impact. For tensile and flexural strengths, molding pressure and duration were important, but for impact strength, they were not. Their mathematical models revealed the important process parameters of the hybrid composites

(ii) This research reveals that 174°C temperature, 6-minute duration, and 34 bar pressure are the best combinations to achieve increased compression molding results. Correlation coefficient values (R^2) of tensile, flexural, and impact strength are 0.96, 0.97, and 0.96, respectively

(iii) Fiber-matrix adhesion was used to confirm the effectiveness of NaOH treatment (5% NaOH for 4 hours). When H_3PO_4 is activated, a reaction occurs between organic molecules and the acid, forming phosphoric and phosphonate linkages. The phosphate groups separate the organic species by being placed into the carbon matrix. After the acid is removed from the matrix, the matrix has a very porous structure

(iv) The activated carbon fibers that arise have a large exterior area, mesopore volume, and broad porous dispersion. Because hemp fibers degrade at a lower temperature than CGF fibers, they disintegrate first during the carbonization stage, resulting in a larger C% and greater surface roughness. The differences in porosity (total, micropore, mesopore) and pore size were extremely modest for all organic fiber-activated carbon specimens

(v) The BET surface area is also related to the surface areas of micropores and mesopores but is inversely proportional to pore size. The SEM discovered non-uniform permeability, confirming the vast pore size dispersion

Data Availability

The data used to support the findings of this study are included within the article. Should further data or information be required, these are available from the corresponding author upon request.

Conflicts of Interest

The authors declare that there are no conflicts of interest regarding the publication of this paper.

Acknowledgments

The authors thank the Saveetha School of Engineering, SIMATS, Chennai, for the technical assistance. The authors appreciate the supports from Ambo University, Ethiopia.

References

[1] V. Ganesan, V. Shanmugam, B. Kaliyamoorthy et al., "Optimization of mechanical properties in saw-dust/woven-jute fibre/polyester structural composites under liquid nitrogen environment using response surface methodology," *Polymers*, vol. 13, 2021.

[2] J. Shen, Y. Min Xie, X. Huang, S. Zhou, and D. Ruan, "Mechanical properties of luffa sponge," *Journal of the Mechanical Behavior of Biomedical Materials*, vol. 15, pp. 141–152, 2012.

[3] S. Kalyana Sundaram, S. Jayabal, N. S. Balaji, and G. Bharathiraja, "Study of chemical and mechanical properties of Dharbai fiber reinforced polyester composites," *Advanced Composite Materials*, vol. 27, no. 1, pp. 107–117, 2018.

[4] K. Gunasekaran, R. Annadurai, and P. S. Kumar, "Long term study on compressive and bond strength of coconut shell aggregate concrete," *Construction and Building Materials*, vol. 28, no. 1, pp. 208–215, 2012.

[5] A. K. Mohanty, M. Misra, and G. Hinrichsen, "Biofibres, biodegradable polymers and biocomposites: an overview," *Macromolecular Materials and Engineering*, vol. 276-277, no. 1, pp. 1–24, 2000.

[6] I. Shah, J. Li, S. Yang, Y. Zhang, and A. Anwar, "Experimental investigation on the mechanical properties of natural fiber reinforced concrete," *J. Renew. Mater.*, vol. 10, no. 5, pp. 1307–1320, 2022.

[7] M. Boopalan, M. Niranjanaa, and M. J. Umapathy, "Study on the mechanical properties and thermal properties of jute and banana fiber reinforced epoxy hybrid composites," *Composites. Part B, Engineering*, vol. 51, pp. 54–57, 2013.

[8] F. Tanasă, M. Zănoagă, C. A. Teacă, M. Nechifor, and A. Shahzad, "Modified hemp fibers intended for fiber-reinforced polymer composites used in structural applications—a review. I. Methods of modification," *Polymer Composites*, vol. 41, pp. 5–31, 2020.

[9] G. Velmurugan, M. Asad Salman, and V. A. Pasha, "Woven hemp and glass fiber hybrid composite - a comparative study on flexural and hardness properties with and without NaOH treatment," *International Journal of Pure and Applied Mathematics*, vol. 119, pp. 1973–1978, 2018.

[10] E. M. J. Salentijn, Q. Zhang, S. Amaducci, M. Yang, and L. M. Trindade, "New developments in fiber hemp (*Cannabis sativa* L.) breeding," *Industrial crops and products*, vol. 68, pp. 32–41, 2015.

[11] P. Rybiński, B. Syrek, M. Masłowski et al., "Influence of lignocellulose fillers on properties natural rubber composites," *Journal of Polymers and the Environment*, vol. 26, no. 6, pp. 2489–2501, 2018.

[12] S. K. Garkhail, R. W. H. Heijenrath, and T. Peijs, "Mechanical Properties of Natural-Fibre-Mat-Reinforced Thermoplastics Based on Flax Fibres and Polypropylene," *Applied Composite Materials*, vol. 7, no. 5/6, pp. 351–372, 2000.

[13] V. Fiore, T. Scalici, and A. Valenza, "Effect of sodium bicarbonate treatment on mechanical properties of flax-reinforced

epoxy composite materials," *Journal of Composite Materials*, vol. 52, no. 8, pp. 1061–1072, 2018.

[14] V. Fiore and L. Calabrese, "Effect of stacking sequence and sodium bicarbonate treatment on quasi-static and dynamic mechanical Properties of Flax/Jute Epoxy-Based Composites," *Materials*, vol. 12, no. 9, p. 1363, 2019.

[15] L. Y. Mwaikambo and M. P. Ansell, "Chemical modification of hemp, sisal, jute, and kapok fibers by alkalization," *Journal of Applied Polymer Science*, vol. 84, no. 12, pp. 2222–2234, 2002.

[16] M. D. Onat, U. Vaidya, and C. Lungu, "Physical adsorption properties of natural fibers and natural fiber based activated carbons for CO2 emissions," in *ECCM 2012- Compos. Venice, Proc. 15th Eur. Conf. Compos. Mater*, pp. 24–28, 2012.

[17] L. Giraldo, D. P. Vargas, and J. C. Moreno-Piraján, "Study of CO2 adsorption on chemically modified activated carbon with nitric acid and ammonium aqueous," *Frontiers in Chemistry*, vol. 8, pp. 1–11, 2020.

[18] A. R. Reed and P. T. Williams, "Thermal processing of biomass natural fibre wastes by pyrolysis," *International Journal of Energy Research*, vol. 28, no. 2, pp. 131–145, 2004.

[19] J. M. Rosas, J. Bedia, J. Rodríguez-Mirasol, and T. Cordero, "HEMP-derived activated carbon fibers by chemical activation with phosphoric acid," *Fuel*, vol. 88, no. 1, pp. 19–26, 2009.

[20] K. J. Silgado, G. D. Marrugo, and J. Puello, "Adsorption of chromium (VI) by activated carbon produced from oil palm endocarp," *Chemical Engineering Transactions*, vol. 37, pp. 721–726, 2014.

[21] X. H. Song, R. Xu, A. Lai, H. L. Lo, F. L. Neo, and K. Wang, "Preparation and characterization of mesoporous activated carbons from waste tyre," *Asia-Pacific Journal of Chemical Engineering*, vol. 7, no. 3, pp. 474–478, 2012.

[22] X. Wang, D. Li, W. Li et al., "Optimization of mesoporous activated carbon from coconut shells by chemical activation with phosphoric acid," *BioResources*, vol. 8, pp. 6184–6195, 2013.

[23] P. T. Williams and A. R. Reed, "High grade activated carbon matting derived from the chemical activation and pyrolysis of natural fibre textile waste," *Journal of Analytical and Applied Pyrolysis*, vol. 71, no. 2, pp. 971–986, 2004.

[24] L. Liu, X. Wang, H. Zou, M. Yu, and W. Xie, "Optimizing synthesis parameters of short carbon fiber reinforced polysulfonamide composites by using response surface methodology," *Polymer Testing*, vol. 59, pp. 355–361, 2017.

[25] M. Buggy, G. Bradley, and A. Sullivan, "Polymer-filler interactions in kaolin/nylon 6, 6 composites containing a silane coupling agent," *Composites. Part A, Applied Science and Manufacturing*, vol. 36, no. 4, pp. 437–442, 2005.

[26] A. W. Verla, M. Horsfall, E. Verla, A. I. Spiff, and O. A. Ekpete, "Preparation and characterization of activated carbon from fluted pumpkin (Telfairia occidentalis Hook. F) seed shell," *Asian journal of natural and applied sciences*, vol. 1, pp. 39–50, 2012.

[27] R. Fu, L. Liu, W. Huang, and P. Sun, "Studies on the structure of activated carbon fibers activated by phosphoric acid," *Journal of Applied Polymer Science*, vol. 87, no. 14, pp. 2253–2261, 2003.

[28] M. Dizbay-Onat, U. K. Vaidya, J. A. G. Balanay, and C. T. Lungu, "Preparation and characterization of flax, hemp and sisal fiber-derived mesoporous activated carbon adsorbents," *Adsorption Science and Technology*, vol. 36, no. 1-2, pp. 441–457, 2018.

[29] G. E. P. Box and D. W. Behnken, "Some new three level designs for the study of quantitative variables," *Technometrics*, vol. 2, no. 4, pp. 455–475, 1960.

[30] O. Perincek and M. Colak, "Use of experimental Box-Behnken design for the estimation of interactions between harmonic currents produced by single phase loads," *International Journal of Engineering Research and Applications*, vol. 3, pp. 158–165, 2013.

[31] M. Balasubramanian, "Application of Box-Behnken design for fabrication of titanium alloy and 304 stainless steel joints with silver interlayer by diffusion bonding," *Materials and Design*, vol. 77, pp. 161–169, 2015.

[32] R. Govindaraju, S. Jagannathan, M. Chinnasamy, and P. Kandhavadivu, "Optimization of process parameters for fabrication of wool fiber-reinforced polypropylene composites with respect to mechanical properties," *Journal of Engineered Fibers and Fabrics*, vol. 9, pp. 126–133, 2014.

[33] R. Akkerman, M. Bouwman, and S. Wijskamp, "Analysis of the thermoplastic composite overmolding process: interface strength," *Frontiers in Materials*, vol. 7, pp. 1–16, 2020.

[34] H. Zhu, Q. Kong, X. Cao, H. He, J. Wang, and Y. He, "Adsorption of Cr (VI) from aqueous solution by chemically modified natural cellulose," *Desalination and Water Treatment*, vol. 57, no. 43, pp. 20368–20376, 2016.

[35] J. M. Dias, M. C. M. Alvim-Ferraz, M. F. Almeida, J. Rivera-Utrilla, and M. Sánchez-Polo, "Waste materials for activated carbon preparation and its use in aqueous-phase treatment: a review," *Journal of Environmental Management*, vol. 85, no. 4, pp. 833–846, 2007.

[36] V. R. G. Dev, J. R. Venugopal, T. S. Kumar, L. R. Miranda, and S. Ramakrishna, "Agave sisalana, a biosorbent for the adsorption of Reactive Red 120 from aqueous solution," *Journal of the Textile Institute*, vol. 101, no. 5, pp. 414–422, 2010.

[37] S. Sekar, S. Suresh Kumar, S. Vigneshwaran, and G. Velmurugan, "Evaluation of mechanical and water absorption behavior of natural fiber-reinforced hybrid biocomposites," *Journal of Natural Fibers*, vol. 19, no. 5, pp. 1772–1782, 2022.

[38] Y. Devarajan, G. Choubey, and K. Mehar, "Ignition analysis on neat alcohols and biodiesel blends propelled research compression ignition engine," *Energy Sources, Part A: Recovery, Utilization, and Environmental Effects*, vol. 42, no. 23, pp. 2911–2922, 2019.

[39] R. Suryanarayanan, V. G. Sridhar, L. Natrayan et al., "Improvement on mechanical properties of submerged friction stir joining of dissimilar tailor welded aluminum blanks," *Advances in Materials Science and Engineering*, vol. 2021, Article ID 3355692, 6 pages, 2021.

[40] S. Justin Abraham Baby, S. Suresh Babu, and Y. Devarajan, "Performance study of neat biodiesel-gas fuelled diesel engine," *International Journal of Ambient Energy*, vol. 42, no. 3, pp. 269–273, 2021.

[41] S. Yogeshwaran, L. Natrayan, S. Rajaraman, S. Parthasarathi, and S. Nestro, "Experimental investigation on mechanical properties of epoxy/graphene/fish scale and fermented spinach hybrid bio composite by hand lay-up technique," *Materials Today: Proceedings*, vol. 37, pp. 1578–1583, 2021.

[42] C. Gautam, Y. Devarajan, W. Huang, L. Yan, H. Babazadeh, and K. M. Pandey, "Hydrogen fuel in scramjet engines - a brief review," *International Journal of Hydrogen Energy*, vol. 45, pp. 16799–16815, 2020.

[43] L. Natrayan and A. Merneedi, "Experimental investigation on wear behaviour of bio-waste reinforced fusion fiber composite laminate under various conditions," *Materials today: proceedings*, vol. 37, pp. 1486–1490, 2021.

[44] Y. Devarajan, B. Nagappan, G. Choubey, S. Vellaiyan, and K. Mehar, "Renewable pathway and twin fueling approach on ignition analysis of a dual-fuelled compression ignition engine," *Energy & Fuels*, vol. 35, no. 12, pp. 9930–9936, 2021.

[45] V. Paranthaman, K. Shanmuga Sundaram, and L. Natrayan, "Influence of SiC particles on mechanical and microstructural properties of modified interlock friction stir weld lap joint for automotive grade aluminium alloy," *SILICON*, vol. 14, no. 4, pp. 1617–1627, 2022.

[46] S. Sanjeevi, V. Shanmugam, S. Kumar et al., "Effects of water absorption on the mechanical properties of hybrid natural fibre/phenol formaldehyde composites," *Scientific Reports*, vol. 11, no. 1, p. 13385, 2021.

[47] D. K. Rajak, D. D. Pagar, P. L. Menezes, and E. Linul, "Fiber-reinforced polymer composites: manufacturing, properties, and applications," *Polymers*, vol. 11, no. 10, p. 1667, 2019.

[48] G. Velmurugan, T. Shaafi, and M. S. Bhagavathi, "Evaluate the tensile, flexural and impact strength of Hemp and flax based hybrid composites under cryogenic environment," *Materials Today: Proceedings*, vol. 50, pp. 1326–1332, 2022.